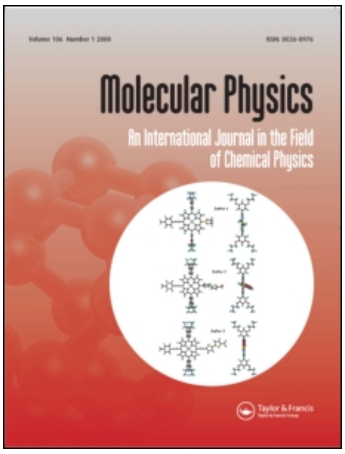

Molecular Physics
Publication details, including instructions for authors and subscription information:
http://www.informaworld.com/smpp/title~content=t713395160

A generalized Langevin algorithm for studying permeation across biological ion channels

Dan Gordon [a]; Vikram Krishnamurthy [b]; Shin-Ho Chung [a]
[a] Research School of Biological Sciences, The Australian National University, Canberra, Australia [b] Department of Electrical Engineering, The University of British Columbia, Vancouver, British Columbia, Canada

Online Publication Date: 01 June 2008

To cite this Article Gordon, Dan, Krishnamurthy, Vikram and Chung, Shin-Ho(2008)'A generalized Langevin algorithm for studying permeation across biological ion channels',Molecular Physics,106:11,1353 — 1361
To link to this Article: DOI: 10.1080/00268970802169145
URL: http://dx.doi.org/10.1080/00268970802169145

Molecular Physics
Vol. 106, No. 11, 10 June 2008, 1353–1361

Taylor & Francis
Taylor & Francis Group

RESEARCH ARTICLE

A generalized Langevin algorithm for studying permeation across biological ion channels

Dan Gordon[a]*, Vikram Krishnamurthy[b] and Shin-Ho Chung[a]

[a]*Research School of Biological Sciences, The Australian National University, Canberra, Australia;* [b]*Department of Electrical Engineering, The University of British Columbia, Vancouver, British Columbia, Canada*

(*Received 11 February 2008; final version received 6 April 2008*)

We present a new leapfrog algorithm for the numerical solution of the generalized Langevin equation (GLE) in the case where the friction kernel is exponentially decaying. Like other leapfrog and Verlet algorithms, our algorithm is second order in velocity and third order in position. It is relatively easy to implement compared with other available algorithms, and would therefore make a good candidate for exploring the effects of finite memory time-scales in situations where modelling the precise functional form of the memory kernel was not important. We have tested this algorithm on a one-dimensional barrier crossing model, and found good asymptotic agreement with limits obtained using Brownian dynamics (BD) simulations, as well as with a theoretical asymptotic limit. We have also used the algorithm to perform a more sophisticated simulation of ion conduction through a KcsA channel. The results are a close match to corresponding results obtained using the Langevin equation, thereby helping to justify the use of Brownian dynamics in KcsA and other similar ion channels.

Keywords: *ab initio*; electronic structure; quantum chemistry; computational chemistry

1. Introduction

The dynamics of systems involving macromolecules surrounded by charged particles and water molecules can be modelled using various degrees of approximation. In order of decreasing computational complexity, we can use quantum mechanical/*ab-initio* methods, classical molecular dynamics (MD), stochastic dynamics (e.g., Brownian dynamics), and continuum methods such as Poisson–Nernst–Planck (PNP) theory [1]. Currently, and for the medium term future, the quantum mechanical methods are only able to handle small systems for short time-scales [1]. While MD can often provide a much more efficient and relatively reliable method to investigate mesoscopic systems, it too is fairly computationally intensive and hence impractical over longer simulation times [1,2]. For example, it is currently unable to be used to statistically calculate conduction rates through typical ion channels. In order to overcome this limitation, stochastic dynamics (SD) may be employed, where only some particles in the system are explicitly modelled, and the rest are treated implicitly through their stochastic influence on the explicitly modelled particles.

The simplest form of stochastic dynamics is Brownian dynamics (BD), in which the stochastic effects are modelled as white noise. This assumption gives rise to the Langevin equation, which is usually numerically solved using either one of two algorithms. The first, due to van Gunsteren and Berendsen [3], is a stochastic analogue of the well-known position Verlet algorithm used in MD. The second, by the same authors [4], is a stochastic analogue of the leapfrog algorithm, also used in MD. Both are third-order finite difference approximations in the position variable.

In some systems, it may be more valid to consider a frequency-dependent noise term. This gives rise to the generalized Langevin equation (GLE), in which the friction and noise terms depend on the history of the system through a memory kernel for the friction. Nilsson and Padró [5], among others [6], have published a hybrid leapfrog/Verlet algorithm that is applicable to a general functional form for the memory kernel. However, the generality of this algorithm requires that each time step must take into account the state of the system at several points in the past. In other words, the algorithm is non-local in time.

We may, as a first-order approximation, wish to consider the effects of system memory by using an exponential functional form for the friction kernel. An exponential friction kernel is convenient because it depends on only two parameters, and it can greatly reduce the computational complexity of the algorithm. In addition, it is a reasonable approximation to the friction kernels of many real systems [7,8], especially

*Corresponding author. Email: dan.gordon@anu.edu.au

ISSN 0026–8976 print/ISSN 1362–3028 online

DOI: 10.1080/00268970802169145
http://www.informaworld.com

when we are not concerned with the dynamics on very short time-scales. If we try to specialize the algorithm of Nilsson and Padró [5] to an exponential friction kernel, then we find that the state of the system at the current time step depends only on its state two time steps ago, and so the algorithm becomes local in time. The algorithm requires that the friction kernel be symmetrical and smooth at $t=0$; this assumption is used in several steps that contain integrals involving Taylor expansions of the kernel about $t=0$. This is not the case for an exponential friction kernel, and one finds that the algorithm loses an order of accuracy when an exponential friction kernel is used. Wan *et al.* [9] have previously published a leapfrog-type algorithm for the generalized Langevin equation, for the special case of an exponential friction kernel. Their algorithm is based on the Langevin dynamics leapfrog algorithm of van Gunsteren and Berendsen [4]. Like other leapfrog algorithms, it is second order in velocity and third order in position. The addition of a finite memory greatly increases the complexity of the mathematical expressions occurring in the algorithm. Therefore, great care must be taken in implementing the algorithm, both in terms of coding accuracy and in dealing with floating point errors.

The algorithm we present here is most influenced by the work of Wan *et al.* [9]. However, it differs in one important respect. At each time step, the algorithm proposed by Wan *et al.* calculates the velocity at the next time step by solving the Langevin equation: there is a frictional contribution to the force that is proportional to the instantaneous velocity. We show that it is possible to instead use the value of the velocity at the beginning of the time step, so that the frictional force during each time step is constant. The result is that we only have to solve Newton's equations of motion at each time step in order to calculate the velocity at the next time step. In this respect, our approach is more like that used by Nilsson and Padró [5]. We show that, like all the other algorithms discussed here, our algorithm is second order in velocity and third order in position.

The advantages of our approach over the previous version [9] are that it is significantly more concise, easier to understand, and easier to implement, while remaining at the same order of accuracy. For example, the mathematical expressions occurring in [9] depend on two time scales—the decay time of the friction memory kernel, and the decay time of the velocity due to the instantaneous component of the friction. The equivalent expressions in our algorithm depend only on the decay time of the friction memory kernel. They are much simpler than the rather complicated expressions occurring in [9], and therefore there should be much less chance of transcription errors and the like during implementation. Also, and perhaps more importantly, because many of these expressions are high order in Δt, one needs to use Taylor expansions to evaluate them in certain parameter regimes, and the single variable functions that occur in our algorithm require significantly less care and tuning in this regard.

2. The leapfrog algorithm

With $v(t)$ denoting the velocity of the particle being modelled and $x(t)$ its position, the GLE is

$$\dot{v}(t) = D(x(t)) + F(t) + S(t). \tag{1}$$

Here, $D(x(t))$ is the deterministic acceleration, determined by a position-dependent potential, $F(t)$ is the frictional acceleration and $S(t)$ is the stochastic acceleration, related to F by the fluctuation dissipation theorem [10]. We assume that $F(t)$ is defined by an exponential friction kernel:

$$F(t) = -K_0 \int_{-\infty}^{t} \mathrm{e}^{-(t-t')/\tau} v(t')\mathrm{d}t'. \tag{2}$$

This is in contrast to the standard Langevin equation, where $F(t) = -\gamma v(t)$.

We shall use a discrete time variable $n \in \mathbb{J}$ to denote the time $t_n := n\Delta t$, and put, for example, $v_n := v(t_n)$, etc. We integrate Equation (1) to obtain an equation for $v_{n+1/2}$ in terms of $v_{n-1/2}$:

$$v_{n+1/2} - v_{n-1/2} = \int_{-\Delta t/2'}^{\Delta t/2} (D(x(t_n + t)) + F(t_n + t) + S(t_n + t))\mathrm{d}t. \tag{3}$$

To obtain an equation for x_{n+1} in terms of x_n, we write

$$v(t_n + t) - v(t_{n+1/2}) = \int_{\Delta t/2}^{t} (D(x(t_n + t')) + F(t_n + t') + S(t_n + t'))\mathrm{d}t', \tag{4}$$

and therefore

$$\begin{aligned} x_{n+1} - x_n &= \int_0^{\Delta t} v(t_n + t')\mathrm{d}t' \\ &= \int_0^{\Delta t} \mathrm{d}t' \left[v_{n+1/2} + \int_{\Delta t/2}^{t'} (D(x(t_n + t'')) + F(t_n + t'') + S(t_n + t''))\mathrm{d}t'' \right] \\ &= v_{n+1/2}\Delta t + \int_0^{\Delta t} \mathrm{d}t' \int_0^{t'-\Delta t/2} (D(x(t_{n+1/2} + t'')) + F(t_{n+1/2} + t'') + S(t_{n+1/2} + t''))\mathrm{d}t''. \end{aligned} \tag{5}$$

In the following sections, we evaluate the integrals of D, F and S that occur in Equations (3) and (5). We aim to calculate v to second order in Δt and x to third order.

3. The deterministic acceleration

Expanding D to first order gives

$$D(x(t_n + t)) = D(x_n) + v_n D'(x_n)t + O(t^2), \tag{6}$$

and hence the deterministic integral occurring in the expression (3) for v is

$$\int_{-\Delta t/2}^{\Delta t/2} D(x(t_n + t))\mathrm{d}t = D(x_n)\Delta t + O(\Delta t^3). \tag{7}$$

The integral occurring in the expression (5) for x is

$$\int_0^{\Delta t} \mathrm{d}t' \int_0^{t'-\Delta t/2} D(x(t_{n+1/2} + t''))\mathrm{d}t'' = \frac{1}{24} v_{n+1/2} D'(x_{n+1/2})\Delta t^3 + O(\Delta t^4). \tag{8}$$

However, if we write[1]

$$\begin{aligned} x_{n+1} &= x_n + v_{n+1/2}\Delta t + \Delta t^3 v_{n+1/2} D'(x_{n+1/2})/24 + \cdots \\ x_{n-1} &= x_n - v_{n-1/2}\Delta t - \Delta t^3 v_{n-1/2} D'(x_{n-1/2})/24 + \cdots \\ &= x_n - v_{n-1/2}\Delta t - \Delta t^3 v_{n+1/2} D'(x_{n+1/2})/24 \\ &\quad + O(\Delta t^4) + \cdots \end{aligned} \tag{9}$$

and add, we obtain

$$x_{n+1} + x_{n-1} = 2x_n + (v_{n+1/2} - v_{n-1/2})\Delta t + O(\Delta t^4) + \cdots, \tag{10}$$

i.e. the term involving D' cancels to third order, and thus we can neglect it and the algorithm will still be at third order.

4. The frictional acceleration

Assume an exponential friction kernel:

$$F(t) = -K_0 \int_{-\infty}^{t} \mathrm{e}^{-(t-t')/\tau} v(t')\mathrm{d}t'. \tag{11}$$

We can make a connection to a known friction coefficient γ by taking the limit as $\tau \to 0$; we find that $K_0 \approx \gamma/\tau$.

Assuming $F(\cdot)$ is analytic around t_n, the Taylor series for F gives

$$F(t_n + t') = F(t_n) + \dot{F}(t_n)t' + O(t'2). \tag{12}$$

We can calculate (e.g. using the Leibniz integral rule) that

$$\dot{F}(t) = -K_0 v(t) - \frac{1}{\tau} F(t), \tag{13}$$

and, therefore, we have

$$F(t_n + t) = F_n - (K_0 v_n + F_n/\tau)t + O(t^2). \tag{14}$$

Thus the friction integral occurring in the expression (3) for v is

$$\int_{-\Delta t/2}^{\Delta t/2} F(t_n + t)\mathrm{d}t = F_n \Delta t + O(\Delta t^3). \tag{15}$$

Note that, to second order, this takes the form of a frictional acceleration that is constant over the time step. This is in contrast to [9], where the frictional acceleration includes an instantaneous component $\xi v(t)$ (with $\xi := K_0\tau(1 - \exp(\Delta t/\tau))$), and at each time step the Langevin equation is solved with this expression as frictional term.

The integral occurring in the expression (5) for x is

$$\int_0^{\Delta t} \mathrm{d}t' \int_0^{t'-\Delta t/2} F(t_{n+1/2} + t'')\,\mathrm{d}t'' = -\frac{1}{24}(F_{n+1/2}/\tau + K_0 v_{n+1/2})\Delta t^3 + O(\Delta t^4). \tag{16}$$

However, using the same argument as was used for D above, we can neglect this term and still keep the algorithm at third order in x.

We also need a way of calculating F_{n+1} from F_n in order to propagate the algorithm. We start by expressing F as a sum over intervals of a single time step:

$$F(t) = -K_0 \sum_{k=0}^{\infty} \int_{-\Delta t/2}^{\Delta t/2} \mathrm{e}^{-((k+1/2)\Delta t - t')/\tau} \times v(t' + t - (k + 1/2)\Delta t)\mathrm{d}t'. \tag{17}$$

Then

$$\begin{aligned} F_{n-1} &= -K_0 \sum_{k=0}^{\infty} \int_{-\Delta t/2}^{\Delta t/2} \mathrm{e}^{-((k+1/2)\Delta t - t')/\tau} \\ &\quad \times v(t_{n-1} + t' - (k + 1/2)\Delta t)\mathrm{d}t' \\ F_n &= -K_0 \sum_{k=0}^{\infty} \int_{-\Delta t/2}^{\Delta t/2} \mathrm{e}^{-((k+1/2)\Delta t - t')/\tau} \\ &\quad \times v(t_n + t' - (k + 1/2)\Delta t)\mathrm{d}t' \\ &= -K_0 \sum_{k=1}^{\infty} \int_{-\Delta t/2}^{\Delta t/2} \mathrm{e}^{-((k+1/2)\Delta t - t')/\tau} \\ &\quad \times v(t_n + t' - (k + 1/2)\Delta t)\mathrm{d}t' \end{aligned}$$

$$
\begin{aligned}
&- K_0 \int_{-\Delta t/2}^{\Delta t/2} \mathrm{e}^{-(\Delta t/2 - t')/\tau} v(t_n + t' - \Delta t/2)\mathrm{d}t' \\
&= -K_0 \sum_{k=0}^{\infty} \int_{-\Delta t/2}^{\Delta t/2} \mathrm{e}^{-((k+3/2)\Delta t - t')/\tau} \\
&\quad \times v(t_n + t' - (k+3/2)\Delta t)\mathrm{d}t' \\
&\quad - K_0 \int_{-\Delta t/2}^{\Delta t/2} \mathrm{e}^{-((1/2)\Delta t - t')/\tau} v(t_n + t' + \Delta t/2)\mathrm{d}t' \\
&= \mathrm{e}^{-\Delta t/\tau} F(t_{n-1}) - K_0 \int_{-\Delta t/2}^{\Delta t/2} \mathrm{e}^{-(\Delta t/2 - t')/\tau} \\
&\quad \times v(t_{n-1/2} + t')\mathrm{d}t',
\end{aligned}
$$

so finally, we have

$$
F_n = \mathrm{e}^{-\Delta t/\tau} F_{n-1} - K_0 \tau (1 - \mathrm{e}^{-\Delta t/\tau}) v_{n-1/2} + O(\Delta t^2), \tag{18}
$$

where we have expanded F to first order in Δt, which is enough keep the algorithm at second order for v and third order for x.

5. The stochastic acceleration

We have, by the second fluctuation-dissipation theorem [10], for $t > 0$,

$$
\langle S(0)S(t)\rangle = \frac{K_0 kT}{m} \mathrm{e}^{-t/\tau}. \tag{19}
$$

It can be shown [9,11] that S satisfies a Langevin equation:

$$
\dot{S}(t) = -\frac{1}{\tau} S(t) + R(t). \tag{20}
$$

Here, R is a continuous time white noise process with

$$
\langle R(0)R(t)\rangle = \frac{2K_0 kT}{m\tau} \delta(t), \tag{21}
$$

where $\delta(t)$ denotes the Dirac delta function. We can solve for S:

$$
S(t + t') = S(t)\mathrm{e}^{-t'/\tau} + W(t, t + t'), \tag{22}
$$

where

$$
W(t_a, t_b) = \int_{t_a}^{t_b} \mathrm{e}^{-(t_b - t)/\tau} R(t)\mathrm{d}t. \tag{23}
$$

In the following, we shall make use of the shorthand notation, for example $W_n := W(t_n,\ t_{n+\Delta t/2})$, where the integral is understood to be over a half time step.

The stochastic integral occurring in the expression (3) for v is

$$
\begin{aligned}
&\int_{-\Delta t/2}^{\Delta t/2} S(t_n + t)\mathrm{d}t \\
&= \int_{-\Delta t/2}^{\Delta t/2} (S(t_n)\mathrm{e}^{-t/\tau} + W(t_n, t_n + t))\mathrm{d}t \\
&= 2\tau S_n \sinh(\Delta t/(2\tau)) + \int_{-\Delta t/2}^{\Delta t/2} W(t_n, t_n + t)\mathrm{d}t \\
&= S_n \Delta t + \int_{-\Delta t/2}^{\Delta t/2} W(t_n, t_n + t)\mathrm{d}t + O(\Delta t^3) \\
&= S_n \Delta t + \int_{-\Delta t/2}^{\Delta t/2} \mathrm{d}t \mathrm{e}^{-t/\tau} \int_{t_n}^{t_n + t} \mathrm{e}^{-(t_n - t')/\tau} R(t')\mathrm{d}t' + O(\Delta t^3),
\end{aligned} \tag{24}
$$

and, integrating by parts,

$$
\int_{-\Delta t/2}^{\Delta t/2} S(t_n + t)\mathrm{d}t = S_n \Delta t + \tau(V_{n-1/2} + Y_n) + O(\Delta t^3), \tag{25}
$$

where V and Y are random variables:

$$
V_{n-1/2} = \int_{t_{n-1/2}}^{t_n} (1 - \mathrm{e}^{(t - t_{n-1/2}))/\tau}) R(t)\mathrm{d}t, \tag{26}
$$

$$
Y_n = \int_{t_n}^{t_{n+1/2}} (1 - \mathrm{e}^{-(t_{n+1/2} - t))/\tau}) R(t)\mathrm{d}t. \tag{27}
$$

The integral occurring in the expression (5) for x can also be obtained in a similar manner by integrating by parts. It is

$$
\begin{aligned}
&\int_0^{\Delta t} \mathrm{d}t' \int_0^{t' - \Delta t/2} S(t_{n+1/2} + t'')\,\mathrm{d}t'' \\
&\quad = S_{n+1/2}(\tau \Delta t - 2\tau^2 \sinh(\Delta t/(2\tau))) + \tau^2 (X_n + Z_{n+1/2}) \\
&\quad = -S_{n+1/2} \Delta t^3/(24\tau) + \tau^2 (X_n + Z_{n+1/2}) + O(\Delta t^5),
\end{aligned} \tag{28}
$$

where the random variables X and Z are defined by

$$
\begin{aligned}
X_n &= \int_{t_n}^{t_{n+1/2}} \left(\mathrm{e}^{(t - t_n)/\tau} - 1 - (t - t_n)/\tau\right) S(t)\mathrm{d}t, \\
Z_{n-1/2} &= \int_{t_{n-1/2}}^{t_n} \left(\mathrm{e}^{-(t_n - t)/\tau} - 1 + (t_n - t)/\tau\right) S(t)\mathrm{d}t.
\end{aligned} \tag{29}
$$

The variables $W_{n-1/2}$, $V_{n-1/2}$ and $Z_{n-1/2}$ are all correlated because they are all integrals of R over the same interval $[n + 1/2, n]$. The covariance matrix elements are

$$
\langle W_{-1/2}^2 \rangle = \frac{K_0 kT}{m} f_1(-\Delta t/(2\tau)), \tag{30}
$$

$$\langle W_{-1/2}V_{-1/2}\rangle = -\frac{2K_0kT}{m}f_2(\Delta t/(2\tau)), \tag{31}$$

$$\langle W_{-1/2}Z_{-1/2}\rangle = \frac{2K_0kT}{m}\mathrm{e}^{-\Delta t/(2\tau)}f_3(\Delta t/(2\tau)), \tag{32}$$

$$\langle V_{-1/2}^2\rangle = \frac{K_0kT}{m}f_4(\Delta t/(2\tau)), \tag{33}$$

$$\langle V_{-1/2}Z_{-1/2}\rangle = -\frac{2K_0kT}{m}f_5(\Delta t/(2\tau)), \tag{34}$$

$$\langle Z_{-1/2}^2\rangle = \frac{K_0kT}{m}f_6(-\Delta t/(2\tau)), \tag{35}$$

where

$$f_1(x) = 1 - \mathrm{e}^{2x}, \tag{36}$$

$$f_2(x) = \cosh(x) - 1, \tag{37}$$

$$f_3(x) = \sinh(x) - x, \tag{38}$$

$$f_4(x) = \mathrm{e}^{2x} - 1 - 2x - 4(\mathrm{e}^x - 1 - x), \tag{39}$$

$$f_5(x) = \cosh(x) - 1 - \frac{1}{2}x^2, \tag{40}$$

$$f_6(x) = 4x\left(\mathrm{e}^x - 1 - x - \frac{1}{2}x^2\right) - \left(\mathrm{e}^{2x} - 1 - (2x) - \frac{1}{2}(2x)^2 - \frac{1}{6}(2x)^3\right). \tag{41}$$

Note that several of these functions are zero to high order in x—for example, the leading term in f_6 is $O(x^5)$. Therefore, care must be taken when numerically evaluating these expressions, and for $x \ll 1$ it may be necessary to use Taylor series expansions.

Similarly, the variables W_n, Y_n and X_n are all correlated because they are all integrals of R over $[n, n+1/2]$. The covariance matrix elements are

$$\begin{aligned}\left\langle W_0^2\right\rangle &= \frac{K_0kT}{m}f_1(-\Delta t/(2\tau)),\\ &= \left\langle W_{-1/2}^2\right\rangle\end{aligned} \tag{42}$$

$$\begin{aligned}\langle W_0Y_0\rangle &= \frac{2K_0kT}{m}e^{-\Delta t/(2\tau)}f_2(\Delta t/(2\tau))\\ &= -\mathrm{e}^{-\Delta t/(2\tau)}\langle W_{-1/2}V_{-1/2}\rangle,\end{aligned} \tag{43}$$

$$\begin{aligned}\langle W_0X_0\rangle &= \frac{2K_0kT}{m}f_3(\Delta t/(2\tau))\\ &= \mathrm{e}^{\Delta t/(2\tau)}\langle W_{-1/2}Z_{-1/2}\rangle,\end{aligned} \tag{44}$$

$$\left\langle Y_0^2\right\rangle = -\frac{K_0kT}{m}f_4(-\Delta t/2\tau), \tag{45}$$

$$\begin{aligned}\langle Y_0X_0\rangle &= \frac{2K_0kT}{m}f_5(\Delta t/(2\tau))\\ &= -\langle V_{-1/2}Z_{-1/2}\rangle,\end{aligned} \tag{46}$$

$$\left\langle X_0^2\right\rangle = -\frac{K_0kT}{m}f_6(\Delta t/(2\tau)). \tag{47}$$

At each half time step, the variables (W, Y, X) or (W, V, Z) may be sampled using the following procedure. Let M be the covariance matrix for the set of variables being sampled. Let L be the lower triangular matrix that gives the Cholesky decomposition of M: $LL^\top = M$. Let $\mathbf{u}$ be a vector of independent, standard normal variables. Then, assuming that $S(t)$ is Gaussian, $L\mathbf{u}$ samples from the required joint distribution. Alternatively, samples could be generated using Gibbs sampling [12].

6. Steps in the algorithm

Assume the current time is t_n. Assume we already have x_n, $v_{n-1/2}$, F_n, S_n and $(W, V, Z)_{n-1/2}$:

(1) Sample the correlated variables $(W, Y, X)_n$
(2) Sample the correlated variables $(W, V, Z)_{n+1/2}$
(3) Let $v_{n+1/2} = v_{n-1/2} + D_n\Delta t + F_n\Delta t + S_n\Delta t + \tau(V_{n-1/2} + Y_n)$, where $D_n := D(x_n)$
(4) Let $S_{n+1/2} = S_n\mathrm{e}^{-\Delta t/(2\tau)} + W_n$
(5) Let $x_{n+1} = x_n + v_{n+1/2}\Delta t - S_{n+1/2}\Delta t^3/(24\tau) + \tau^2(X_n + Z_{n+1/2})$
(6) Let $F_{n+1} = \mathrm{e}^{-\Delta t/\tau}F_n - K_0\tau(1 - \mathrm{e}^{-\Delta t/\tau})v_{n+1/2}$
(7) Let $S_{n+1} = S_{n+1/2}\mathrm{e}^{-\Delta t/(2\tau)} + W_{n+1/2}$
(8) Let $n \to n+1$, re-label variables accordingly, and go to step 1.

6.1. *Initialization of the algorithm*

Suppose we know x and v at $t = 0$.

One strategy for simulation would be to simulate the system for some prescribed time interval using the Langevin equation, while keeping track of the frictional force F and S, and then switch to the GLE.

In practice, it is simpler to set $F_0 = -\gamma v_0$ if the system is over-damped i.e. $\tau \ll 1/\gamma$, or to set $F_0 = -K_0\tau(1 - \mathrm{e}^{-\Delta t/\tau})v_0$ if the system is under-damped. S_0 is sampled from a Gaussian distribution with zero mean, and variance given by Equation (19). $(W, V, Z)_{-1/2}$ are sampled as described above. $v_{-1/2}$ is calculated as follows:

$$v_{-1/2} = v_0 - D_0\Delta t/2 - F_0\Delta t/2 - S_0\Delta t/2 + O(\Delta t^2). \tag{48}$$

The algorithm can then proceed as per normal.

7. Numerical results

We present two examples motivated by modelling the permeation of ions in biological membrane ion channels.

7.1. *Example 1: Conduction across a potential barrier*

In this example, we consider a particle moving in a one-dimensional potential consisting of a Gaussian potential barrier flanked by a Gaussian potential well on either side. The particle will spend much of its time in one or the other of the wells, but may occasionally cross the barrier from one well to the other. We refer to this as a crossing, and we refer to the moment that the particle crosses the top of the barrier as a microscopic crossing. We are interested in the rate of crossings. This model could, for example, be used as a simplified representation of the passage of ions though an ion channel, from one binding site to another.

We can use statistical mechanics to calculate the rate for the particle to cross the top of the barrier as a function of the equilibrium linear density at a reference position, say in one of the wells. It can be shown that

$$J_1 = \rho_0 \sqrt{\frac{k_B T}{m}} \exp\left(-\frac{U(z_1) - U(z_0)}{k_B T} \right), \qquad (49)$$

where J_1 is the average current across the top of the barrier (at z_1), ρ_0 is the equilibrium linear density at the reference position z_0 (which is most conveniently taken at the bottom of one of the wells), and $U(z)$ is the potential.

This is the microscopic rate of barrier crossings. The actual observed barrier crossing rate may be less than this value, because during each full crossing from one one well to the other, the top of the barrier may be traversed more than once. The rate is further reduced (by a factor of 2, in the diffusive limit) by the fact that the particle will end up on the same side of the barrier that it came from if it happens to pass across the top of the barrier an even number of times before falling back into a well. This kind of behaviour is characteristic of the particle diffusing across the barrier as opposed to crossing it ballistically.

Increasing the decay time for the friction kernel will increase the decay time for the velocity autocorrelation function, and therefore should increase the mean free path length at a given velocity. If we increase the decay time enough, we might expect the particle to be able to traverse the barrier in a nearly ballistic manner. In this regime, the current across the barrier should approach its theoretical maximum value.

As a test of our algorithm, we investigate this argument by keeping the friction coefficient $\gamma \approx K_0/\tau$ constant while varying the memory time-scale τ. The results are presented in Figure 1. The parameters were chosen to allow the full effect of the exponential friction kernel to be illustrated over a reasonable parameter range. The barrier is 7 kT high, with a 1 Å standard deviation. The barrier sits at the bottom of a deep (25 kT), flat-bottomed potential well of width 10 Å; this conveniently provides wells on either side of the barrier, while preventing the particle from escaping to infinity. The mass of the particle is 39 AMU. The time step is 1 fs.

As expected, the average current across the barrier approaches the result for the Langevin equation for short memory decay times. As the decay time is increased, the current increases, and for very long decay times it appears to approach the theoretical maximum value given above.

(A similar effect can be seen when we solve the Langevin equation, varying γ. As $\gamma \to 0$, the mean free path length increases until each microscopic crossing corresponds to a crossing proper—hence the current should increase toward the theoretical maximum given above. We have done this calculation, and found that this is indeed the case.)

7.2. *Example 2: Conduction of ions through the KcsA channel*

In the past, BD simulations have been widely used to elucidate the mechanisms of ion permeation across biological ion channels [13]. Here we compare some of the salient properties of permeation dynamics deduced by using BD with those obtained by using the GLE with various memory decay times (τ).

To make these comparisons, we select the KcsA potassium channel, whose crystal structure has been determined by Doyle *et al*. [14]. The radius of the pore is expanded to 5 Å at the internal end of the channel using a cylindrical repulsive potential in molecular dynamics. The selectivity filter is also expanded slightly such that the minimum radius is 1.4 Å, as described previously by Chung *et al*. [15]. To carry out stochastic dynamics simulations, we first place in three-dimensional space all the atoms forming the potassium channel at the centre of the assembly, and assign the charge on each atom. Then, a large cylindrical reservoir of 30 Å radius with a fixed number of K^+ and Cl^- ions is attached at each end of the channel to mimic the extracellular and intracellular space. The membrane potential is imposed by applying a uniform electric field across the channel.

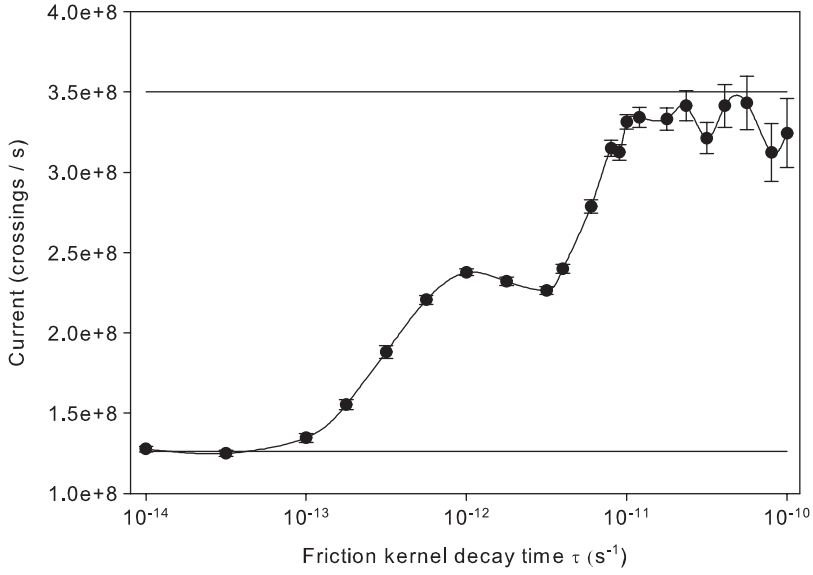

Figure 1. The current across a barrier vs. the friction decay constant τ. The top horizontal line marks the theoretical maximum current as calculated from Equation (49), and the bottom horizontal line marks the measured value when the Langevin equation is solved. The current appears to have two asymptotes: for $\tau \to 0$, the current approaches the calculated result for the Langevin equation, as one would expect, and at high τ, the current approaches the theoretical maximum given in Equation (49). We have also confirmed that this upper limit matches the current when the Langevin equation is solved with $\gamma \to 0$. Error bars in this and the following figures have a length of 2 s.e.m.

The diffusion coefficient we use for K^+ in the reservoirs is $1.96 \times 10^{-9}\,m^2\,s^{-1}$. The value is reduced to 0.1 of the bulk value in the narrow selectivity filter and 0.5 of the bulk value elsewhere in the channel, as determined by molecular dynamics calculations [16]. For further details of stochastic dynamics simulations, see Hoyles *et al*. [17].

To increase the efficiency of our simulations, ions in the reservoirs are always modelled using Brownian dynamics, with a long time step of 100 ns. In the bulk solvent region of the reservoirs, the dynamics are expected to be adequately described as a random walk in position space, and hence there is no need to use the GLE in these regions. Any difference in conduction due to the use of the GLE rather than Brownian dynamics will occur inside the pore region. In the pore region, we use a 2 fs time step for the BD simulations, and 1 fs is used for GLE. The 2 fs time step has been found to be the best choice for BD, since inside the channel the ions experience rapidly changing potentials, and furthermore an accurate simulation of the dynamics is more critical in this region. For the GLE, we chose to use a smaller 1 fs time step, to take into account the fact that a greater 'clumpiness' in the temperature of the ions can lead to extended periods of increased temperature.

The current–voltage–concentration profiles of the KcsA potassium channel as constructed with BD are a close match to those constructed with the GLE algorithm outlined here. The three memory decay times we use for GLE are 10^{-14}, 10^{-13} and 10^{-12} s. In Figure 2(a), the current–voltage curve obtained with the decay memory time of 10^{-12} is superimposed on that obtained with BD simulations. For clarity, the curves obtained with $\tau = 10^{-14}$ and 10^{-13} s are omitted from the graph, as these graphs' τ are similar to the curve for $\tau = 10^{-12}$ s. Similarly, the conductance–concentration curves derived from BD and GLE are a close match, as illustrated in Figure 2(b). In the conducting state, the channel is occupied by on average three resident ions, two in the narrow selectivity filter and one near the intracellular gate of the channel. The distributions of ions in the channel determined from the two different algorithms are also the same (data not illustrated here).

We conclude that the permeation mechanisms deduced from BD, in which random forces acting on ions are assumed to be memory-less, do not differ appreciably from those deduced from the GLE algorithm. A potassium ion in the extra- or intracellular space sees a deep energy well created by charged residues and dipoles in the channel protein. The energy well created by these moieties, reaching a depth of nearly 30 kT, attracts three potassium ions. Once the channel is occupied by the resident ions, the energy barrier that an ion at a given binding site needs

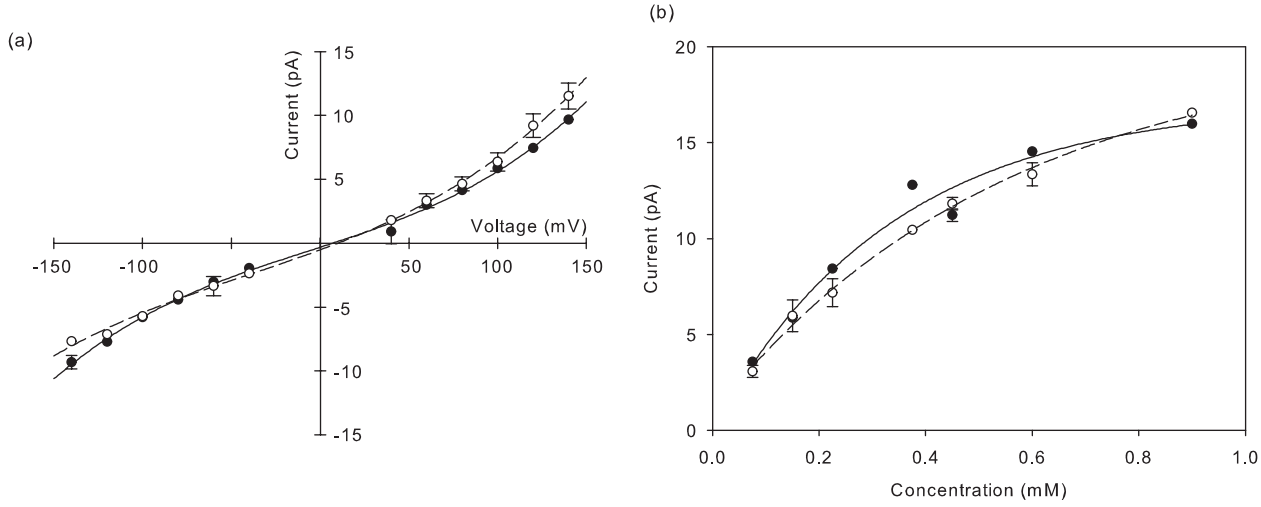

Figure 2. The current–voltage-concentration profiles derived with BD simulations and the GLE algorithm. (a) The current–voltage relationship obtained with BD simulations (filled circles) is superimposed on the relationship derived with the GLE algorithm (open circles) with the memory decay time of 10^{-12} s. (b) The currents at various symmetrical KCl concentrations in the reservoirs obtained with BD simulations are measured at a fixed applied potential of -196 mV (filled circles). Superimposed are the currents measured under identical conditions with the GLE algorithm with the memory decay time of 10^{-13} s. The data points are fitted with the Michaelis–Menten equation. Error bars are not shown when they are smaller than the data points.

to surmount to move to the next binding site becomes relatively small, only a few kT [18]. Thus, the permeation dynamics gleaned from BD simulations are shown to be reliable, and nearly the same as that obtained using the more sophisticated algorithm.

8. Concluding remarks

We have presented a new algorithm for numerically solving the generalized Langevin equation, in the special case where the friction kernel is exponential. Like other algorithms for solving the GLE, our algorithm is second order in velocity and third order in position. We believe that our algorithm is distinguished by its simplicity of implementation. It would make a good choice in situations where it was desired to investigate time-scale effects of a finite memory kernel, without being too concerned about the precise functional form of the kernel.

We have tested the algorithm on a one-dimensional barrier crossing model. The results are asymptotically consistent with results obtained using Brownian dynamics, and also with a simple theoretical expression.

We have gone on to use the algorithm to numerically solve the dynamics of a more sophisticated three-dimensional model of the KcsA ion channel. The resulting current versus voltage and current versus concentration curves are a very close match to those obtained using Brownian dynamics over a range of time-scales for the memory kernel. These results therefore help to justify the use of Brownian dynamics in other similar cases.

Note

1. Here, we use the fact that the change in v over a time step is $O(\Delta t)$. This is obvious in the case of the contributions for the deterministic and frictional acceleration. When we later consider the stochastic acceleration, we need to consider that there is a contribution from two uncorrelated random variables (see Section 5). It turns out that both of these have a variance that goes as $O(\Delta t^2)$.

References

[1] S. Kuyucak, O.S. Andersen, and S.H. Chung, Rep. Prog. Phys. **64**, 1427 (2001).
[2] B. Roux, Biophys. J. **77**, 139 (1999).
[3] W. van Gunsteren and H.J.C. Berendsen, Molec. Phys. **45** (3), 637 (1982).
[4] W. van Gunsteren and H.J.C. Berendsen, Molec. Simul. **1**, 173 (1988).
[5] L.G. Nilsson and J.A. Padró, Molec. Phys. **71** (2), 355 (1990).
[6] D.E. Smith and C.B. Harris, J. Chem. Phys. **92**, 1304 (1990).
[7] T. Başt\u{g} and S. Kuyucak, Chem. Phys. Lett. **401**, 175 (2005).

[8] R. Rey, E. Guardia, and J.A. Padro, J. Chem. Phys. **97**, 8276 (1992).
[9] S.Z. Wan, C.X. Wang, and Y.Y. Shi, Molec. Phys. **93** (6), 901 (1998).
[10] R. Kubo, Rep. Prog. Phys. **29**, 255 (1966).
[11] H. Mori, Prog. Theor. Phys. **34** (3), 399 (1965).
[12] S.M. Ross, *Simulation* (Academic Press, Orlando, FL, 2002).
[13] V. Krishnamurthy and S.H. Chung, Proc. IEEE **95**, 853 (2007).
[14] D.A. Doyle, J.M. Cabral, R.A. Pfuetzner, *et al.*, Science **280**, 69 (1998).
[15] S.H. Chung, T.W. Allen, and S. Kuyucak, Biophys. J. **83**, 263 (2002).
[16] T.W. Allen, S. Kuyucak, and S.H. Chung, Biophys. Chem. **86**, 1 (2000).
[17] M. Hoyles, S. Kuyucak, and S.H. Chung, Phys. Rev. E **58**, 3654 (1998).
[18] S.H. Chung, Biophys. J. **77**, 2517 (1999).